Z. Kristallogr. **221** (2006) 402–411 / **DOI** 10.1524/zkri.2006.221.5–7.402

Reflections on symmetry and formation of axial quasicrystals

Walter Steurer*

Laboratory of Crystallography, Department of Materials, ETH Zurich, Wolfgang-Pauli-Strasse 10, 8093 Zurich, Switzerland

In commemoration of the 100th anniversary of Fritz Laves' birthday

Received November 21, 2005; accepted February 10, 2006

Quasicrystals / Decagonal / Heptagonal / Geometrical growth model / Al–Co–Ni

Abstract. Some ideas are presented on the geometrical factors governing structure and formation of axial quasicrystals with 5- and 7-fold symmetry, respectively. First, the importance of thin atomic layers is discussed for the growth of decagonal quasicrystals. They are the only long-range ordered structural units carrying information on the local non-crystallographic symmetry of the constituent clusters. Second, the consequences of local polysynthetic twinning for the formation of pentagonal and heptagonal quasicrystals are demonstrated. Third, the special relationship of the β-phase, $(Co,Ni)_{1-x}Al_{1+x}$, to the decagonal phase and its periodic average structure is discussed as well as its role as template for the formation and growth of decagonal Al–Co–Ni.

Introduction

Fifty years ago, Fritz Laves presented his ideas on the factors governing the structure of metals (Laves, 1956). He came to the conclusion that "as a consequence of these principles (space-, symmetry- and connection-principle) the stoichiometrical formulae of intermetallic compounds are frequently fixed rather by the geometrical properties ... than by the formal valencies of the components". By Laves's principles some peculiarities of structures could be explained that were not covered by "the three factors considered by Hume-Rothery (a) size factor, (b) electrochemical factor, (c) valence electron concentration".

It is well known that in the case of quasicrystals (*QCs*) size factor (Elser, 1985; Chen *et al.*, 1987; Guo *et al.*, 2002) and valence electron concentration (cf. Trambly de Laissadiere *et al.*, 2005) play a crucial role for their stability. All these parameters, however, neither explain the observed symmetries and structures of *QCs* nor show how they form. Therefore, we will discuss the importance of further geometrical parameters, local twinning, thin atomic layers and the periodic average structure, for symmetry, formation and growth of decagonal *QCs* (*DQCs*). The following points will be addressed:

1. What favors quasiperiodicity over periodicity?
2. Why are stable *QCs* always 5-fold symmetric?
3. How do *DQCs* grow, what are the real matching or overlapping rules?

Periodicity *versus* quasiperiodicity

Why are crystal structures almost always periodic and in what cases do they get quasiperiodic? What are the fundamental differences between periodic and quasiperiodic structures? Which parameters favour quasiperiodicity?

Any crystal, be it periodic or aperiodic, is built from a finite number of different basic structural units (consisting of atoms, ions, molecules, complex ions, clusters ...) or unit cells contrary to amorphous solids and liquids. Consequently, these basic units have to be repeated in a given order over and over again. This forms the physical basis of the principle of repetitivity.

If there are not too strong constraints based on non-crystallographic symmetries or special construction rules of the basic structural units, repetitivity is usually realized in form of translational periodicity. Even fullerene molecules or viruses with almost perfect icosahedral symmetry, for instance, form periodic crystal structures. So does the great many of intermetallic phases built from icosahedral coordination polyhedra (Daams, Villars, 2000).

However, if there are at least two different unit cells, quasiperiodicity can be forced by special matching rules even if the unit cells show crystallographic symmetry (Fig. 1).

In case of structures with translational symmetry, repetitivity corresponds to additivity on the scale of unit cells. Additivity is the natural growth principle of simple crystal structures with isotropic atomic interactions such as they exist between atoms of the noble gases or some metallic elements. The additivity principle under the constraint of maximum packing density leads to either cubic (*ccp*) or hexagonal (*hcp*) close sphere packings. Although the packing density is in both cases the same, $\pi/\sqrt{18} = 0.74\ldots$, the shape of the coordination polyhedra differs from the first shell up. The long-range order of the two structure

* e-mail: steurer@mat.ethz.ch

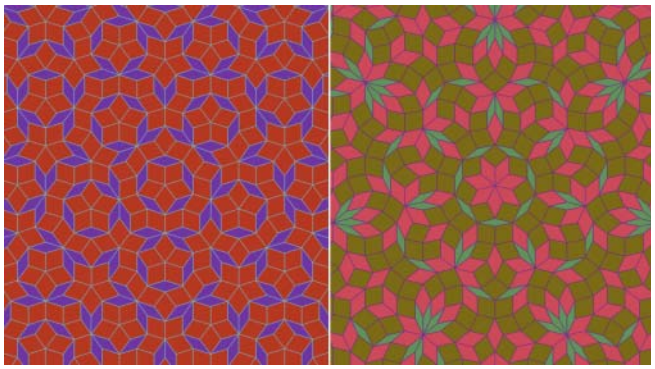

ⓐ ⓑ

Fig. 1. (**a**) Pentagonal and (**b**) heptagonal tiling generated by the dual-grid method (Weber, 1999). The pentagonal tiling (Penrose tiling) is based on two different rhombic unit tiles, the heptagonal tiling on three.

types is different as well. This is reflected in the distribution of close-packed atomic planes, which are stacked along [001] in case of *hcp* and perpendicular to the facets of an octahedron {111} in case of *ccp*. It is obvious that large energetically favorable multi-shell clusters with octahedral symmetry would prefer cubic close packing.

Translational periodicity as geometrical building principle pays off energetically in the case of small-unit-cell structures. Particularly, if the Friedel oscillations of the atomic pair potentials are in registry with the lattice period. The benefits of periodicity are not so obvious in the case of complex metallic alloys (*CMAs*), *i.e.* large-unit-cell structures with lattice parameters far beyond the interaction potentials of single atoms, which are less than ≈10 Å in case of Al, Co, Ni, for instance (Widom *et al*., 2000).

The formation of *CMAs* is easier to understand if they result from interactions of mutually incommensurate subsystems competing in a structure. Even if the basic unit cell is very small and the underlying modulation principle simple, rather large lattice parameters can be the consequence. For instance, Au−Cu forms anti-phase domain structures with modulation wavelengths up to ≈80 Å, continuously varying with the electron concentration (Sato and Toth, 1961; 1962).

Another kind of incompatibility arises, if the structural building units have non-crystallographic symmetries and periodic packing becomes less efficient than quasiperiodic one. This does not only refer to the packing density but also to the number of realizations of, for instance, energetically favorable clusters (Jeong, Steinhard, 1994; Steinhardt *et al*., 1998).

The question is why aperiodic structures are formed instead of large approximants, why periodicity is sacrificed. Approximants are either periodic crystal structures based on the same structural units (clusters) as *QCs* or commensurate superstructures of a common basic structure in case of incommensurately modulated structures (*IMSs*), respectively. *QCs* are often accompanied by approximants with slightly different stoichiometry. However, these are never large-unit-cell approximants. And a devil's staircase has never been found, *i.e.* a series of higher and higher approximants, as it is known for some *IMSs* (Cummins, 1990). Commensurate superstructures are lock-in phases, and it is not possible to move the modulation wave through a commensurately modulated crystal without changing its energy as it is the case for *IMSs*. For a *QC*, it is not just a change in the period of a modulation wave that makes an approximant to a *QC*. *QCs* represent already a kind of lock-in state regarding symmetry, approximants break the symmetry. While *IMSs* have a lower symmetry than their periodic average structure *(PAS), QCs* have a higher one. A continuous variation of the wavelength of an *IMS*, for instance by variation of temperature, produces continuously changing lattice parameters. Rational approximants of a *QC* change their lattice parameters with increasing order stepwise, by powers of τ in the case of *DQCs,* for instance.

Consequently, there must be a fundamental difference even between high-order approximants and *QCs* that favors *QCs* significantly. The advantage of an approximant is its periodicity and therewith its simpler construction principle, however, only if it is an low-order approximant. The advantage of a *QC* is its higher symmetry that is adapted to the symmetries of the constituent clusters. And there must be a simple construction principle compared with a high-order approximant based upon that higher symmetry.

Of course, in a discussion on the stability of *QCs* versus that of approximants, the configurational entropy has also to be taken into account. Let us consider a structure just on the scale of the unit cell. In case of periodic structures, there is only one unit cell, no disorder of uniquely decorated cells is possible, the resulting entropy is zero. In case of quasiperiodic structures (tilings), the quasilattice has at least two unit cells. Randomization of the quasilattice and therewith of the distribution of the different unit cells can increase the entropy significantly (see, for instance, Elser, 1996; Gähler *et al*., 2002). If the quasilattice is randomized under the constraint that the average structure remains quasiperiodically, *i.e.* the perpendicular-space fluctuations of the cutting space remain bounded, then the diffraction pattern shows still sharp Bragg reflections accompanied by some diffuse scattering.

The role of symmetry

2D and 3D lattice periodicity is compatible with $n^c = 1$-, 2-, 3-, 4- and 6-fold rotational symmetry (*i.e.* crystallographic symmetry). If one lattice point is a point of global n^c-fold symmetry then all other lattice points are such as well. Rotation around any of these points brings the lattice n^c-times into coincidence with itself. On the contrary, a 2D or 3D quasilattice cannot contain more than a single point of global non-crystallographic n^{nc}-fold symmetry.

All known stable *QCs* show 5-fold, 10-fold or icosahedral symmetry (cf. Steurer, 2004, and references therein). There are a few reports on *QCs* with 8- or 12-fold symmetry. However, they are metastable and/or of poor quality. Not a single *QC* with any other non-crystallographic symmetry has ever been reported. Why? For the hypothetical case of 2D structures, it has been shown that only *QCs* based on quadratic irrationalities, $a + b\sqrt{c}$ (*a, b, c*... rational numbers), should be energetically stable (Levitov, 1988). Consequently, only *QCs* with 5-, 8-, 10- or 12-fold

symmetries would be allowed. 3D *QCs*, however, could also be based on cubic irrationalities leading to 7- and 9-fold symmetry, respectively (Pelantova, Twarock, 2003). The 2D quasiperiodic part of a *QC* with axial *n*-fold symmetry can be described as cut of a 4D hypercrystal in case of quadratic irrationalities and of a 6D hypercrystal in case of cubic irrationalities. The *n*D embedding space consists of the physical or parallel space and the perpendicular space orthogonal to it, $\mathbf{V} = \mathbf{V}^{\parallel} \oplus \mathbf{V}^{\perp}$ (cf. Steurer, Haibach, 1999b). In the case of a 6D embedding space, the dimension of the perpendicular space would be higher than that of the physical space. There would be two types of phason fields instead of just one for the actually known *QCs* (Hu *et al.*, 1994).

It is not too surprising that 5-fold symmetry is *the* symmetry of *QCs,* if one takes into account that icosahedral coordination is the most frequent atomic environment type (*AET*) in intermetallic phases (Daams, Villars, 2000). However, since icosahedra cannot be packed without gaps, they are distorted and/or mixed with other *AETs*. Furthermore, not only in solids but also in undercooled metallic melts icosahedral short-range order may not be the exception (Kelton, 2003).

What about *AETs* with, for instance, 7-fold symmetry? First of all there do not exist regular or semiregular polyhedra (Platonic or Archimedian solids) with more than 5-fold symmetry. However, polyhedra with only axial *n*-fold symmetry are possible for arbitrary *n.* Indeed, (distorted) seven-membered rings are very common in ternary borides. The *oP*24-$YCrB_4$ structure type (Dub *et al.*, 1985), for instance, with more than 90 known representatives, is built from heptagonal bipyramids decorating the vertices of a tiling of squashed hexagons. The heptagonal bipyramids consist of a heptagonal boron ring capped by the large rare earth atoms. The voids left by the heptagonal bipyramids correspond to pentagonal bipyramids capped by the smaller transition metal (TM) atoms.

Why then are heptagonal quasicrystals not known? A tiling with 7-fold symmetry can be constructed by the dual-grid method as easily as one with 5-fold symmetry (Fig. 1). It gets more complicated, however, if we try to construct a structure based on a cluster with 7-fold symmetry. We demonstrate this on the example of local polysynthetic twinning of a pentagonal and a heptagonal cluster (*e.g.*, pentagonal and hexagonal bipyramids, respectively). The first pentagon *P* (nucleus) is twinned along its edges: $P + 5P \rightarrow P5P$. The twinning is repeated at the edges of the τ^2-times larger (in diameter) aggregates: $P5P + 5P5P$

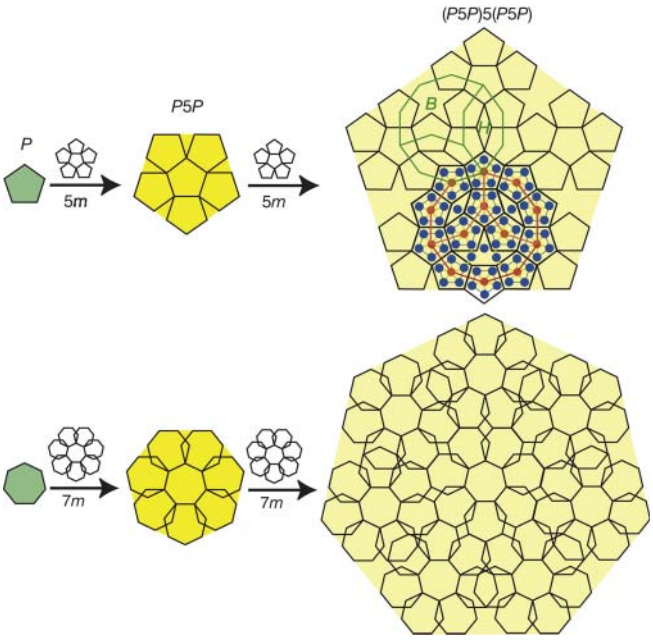

Fig. 2. Fractal *N*-grammal growth model for $n = 5$ and $n = 7$. The growth takes place by twinning along the free edges of the *n*-gons and clusters of *n*-gons. In case of the pentagon, after the second twinning cycle, decagons (green line) appear, consisting of two hexagons, *H*, and one boat tile, *B,* that are typical for decagonal quasicrystals. A decagon of the type found in decagonal Al−Co−Ni, decorated with Al (blue) and TM (red) atoms, is shown. In case of heptagons, even the first twinning cycle leads to overlapping of neighboring heptagons.

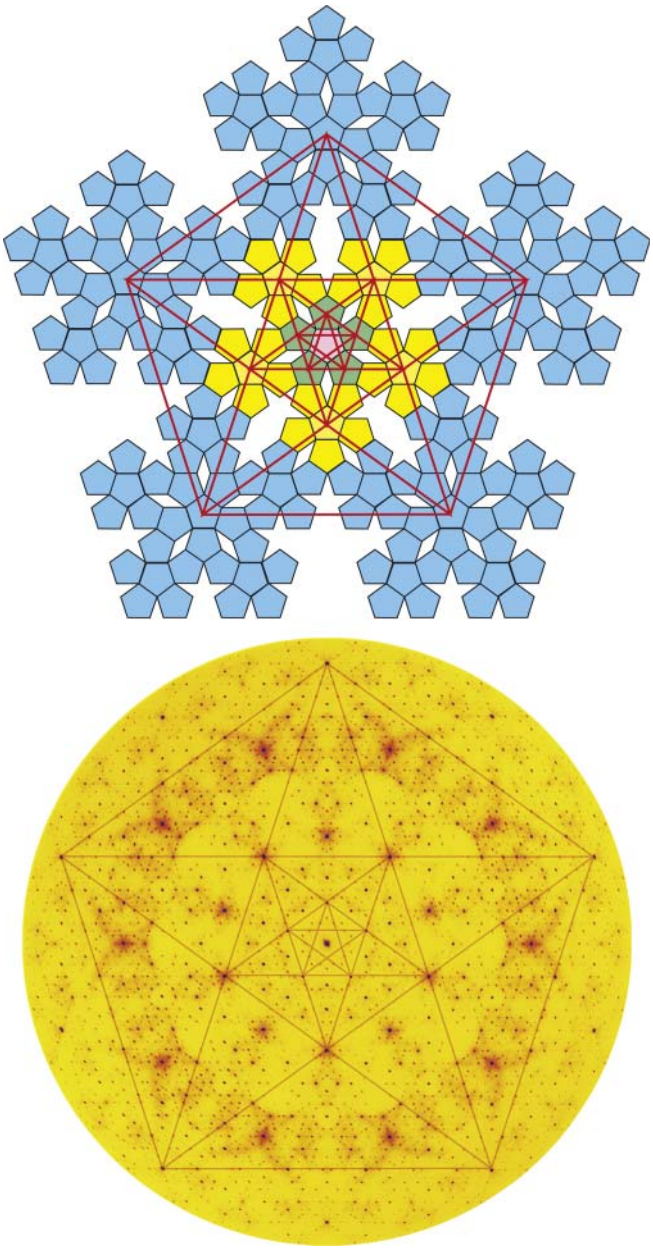

Fig. 3. Pentagrammal symmetry (cf. Janner, 1992) in direct and reciprocal space (diffraction pattern of decagonal Al−Co−Ni).

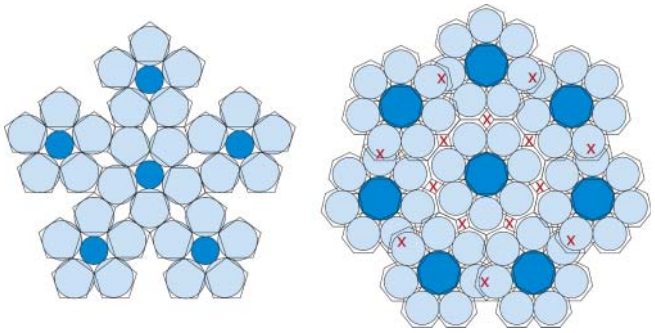

Fig. 4. *N*-grammal growth model for $n = 5$ and 7, respectively. The n-gons are occupied by atoms. The atomic sizes are chosen so that the n atoms around the central atom touch each other and the central atom as well. The red crosses mark the mismatch regions.

$\rightarrow$ (*P5P*) 5(*P5P*) (Fig. 2) and so forth. During crystal growth twinning means that the atomic structure grows until a certain termination plane (twin plane) is reached. Then further growth continues by repeating the structure formation process in the reverse direction.

What we obtain by this kind of local polysynthetic twinning of a pentagon is a fractal pentagon-rhomb tiling with pentagrammal symmetry (cf. Janner, 1992), which is always present in diffraction patterns of *DQCs* (Fig. 3). There are no overlaps of pentagons, however, there are some spandrels left that can be filled by further pentagons and boats. We also see, starting from a certain size, patches of tiles (clusters consisting of hexagons, *H,* and boats, *B,* see upper right drawing of Fig. 2) can be identified that cover the tiling.

The local twinning procedure applied to heptagons leads already in the first coordination shell to overlaps (Fig. 2). If we decorate the pentagons and heptagons by atoms in an appropriate way (Fig. 4) then we do not have packing problems in case of the pentagonal clusters. In contrast, atoms of the heptagonal clusters partially overlap and leave some empty space as well (marked by red crosses in Fig. 4). This makes a further growth in this way impossible.

Higher-dimensional description of *QCs*

The simplest example of a *QC* is the 1D Fibonacci sequence (*FS*). It can be generated either by substitution rules or as a cut of a 2D hypercrystal (Fig. 5). The substitution rule $\sigma : S \mapsto L$, $L \mapsto LS$ replaces a letter S by L and the letter L by the word LS (Tab. 1) (cf. Luck *et al.*, 1993). An infinite *FS* remains invariant under this substitution rule. The Fibonacci numbers F_{n+1} and F_n, with $F_n = F_{n-1} + F_{n-2}$, give the frequency of L and S, respectively, in the chain. The limit of the sequence of their ratios

$$\lim_{n\to\infty} \frac{F_{n+1}}{F_n} = \tau = 1.618\ldots = (1+\sqrt{5})/2 = 2\cos(\pi/5)$$

as n approaches infinity is the golden mean τ. The number τ is also the solution of the quadratic algebraic equation $\tau^2 - \tau - 1 = 0$.

If we assign to L and S long and short intervals with the ratio

$$\frac{L}{S} = \frac{LS}{L} = \frac{LSL}{LS} = \frac{LSLLS}{LSL} = \ldots = \tau$$

Table 1. Generation of the Fibonacci sequence by the substitution rule σ. The frequency of letters L and S is given by the respective Fibonacci numbers F_{n+1} and F_n.

n	Words	Number of S, F_n	Number of L, F_{n+1}	F_{n+1}/F_n
0	L	0	1	$^0/_1 = 0$
1	LS	1	1	$^1/_1 = 1$
2	LSL	1	2	$^2/_1 = 2$
3	$LSLLS$	2	3	$^3/_2 = 1.5$
4	$LSLLSLSL$	3	5	$^5/_3 = 1.666\ldots$
5	$LSLLSLSLLSLLS$	5	8	$^8/_5 = 1.6$
	...			
8	...			$\tau = 1.618\ldots$

then we get a quasilattice, which is invariant under scaling with τ^n. Decoration of the vertices with atoms gives a simple model of a 1D quasiperiodic structure.

Embedding the *FS* in 2D space allows its description as 1D cut of a periodic 2D hypercrystal (cf. Steurer, Haibach, 1999b, and references therein) (Fig. 5). The lattice is spanned by the basis vectors $\mathbf{d}_1$, $\mathbf{d}_2$. The slope of $\mathbf{d}_1$ is equal to $-\tau$. The vertices of the *FS* are generated where the physical space, $\mathbf{V}^{\|}$, cuts the atomic surfaces (red and green line segments in Fig. 5). The size of the atomic surface results from the projection of a 2D unit cell upon the perpendicular space. The frequency of distances L and S is proportional to the height of the blue and green shaded

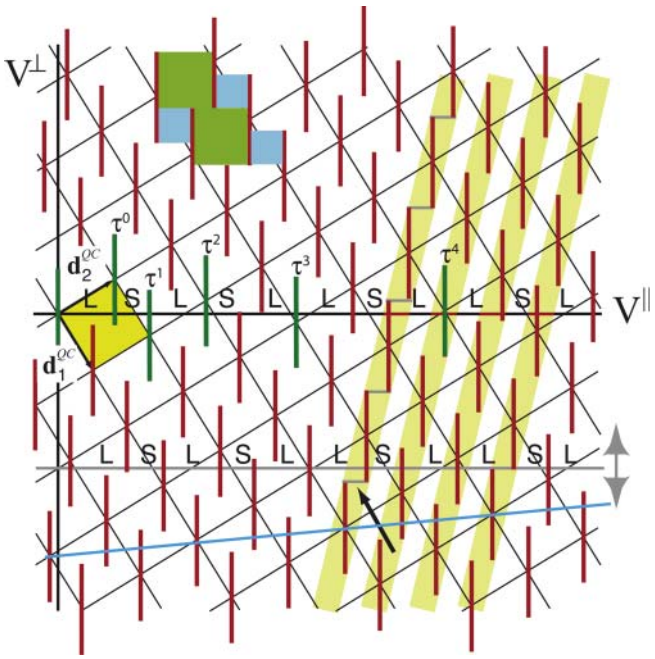

Fig. 5. 2D description of the *FS*. The 2D unit cell (marked yellow) is spanned by the vectors $\mathbf{d}_1$ and $\mathbf{d}_2$. The 1D quasiperiodic *FS* results from the cut of the atomic surfaces (red and green bars) of the 2D hypercrystal structure with the physical space $\mathrm{V}^{\|}$. The arrow marks a phason flip ... *SL* ... $\Leftrightarrow$ ... *LS* ... Distances of type L are marked by green, S by blue areas. By oblique projection of the atomic surfaces upon the physical space, the 1D *PAS* (red horizontal line segments) of the *FS* is obtained. The green line segments have distances $\tau^n L$ from the origin and correspond to pseudo-mirror planes of the 1D *FS*. The inclined blue line cuts the periodic $^2/_1$ approximant ... *LSL* ... out of the hypercrystal structure.

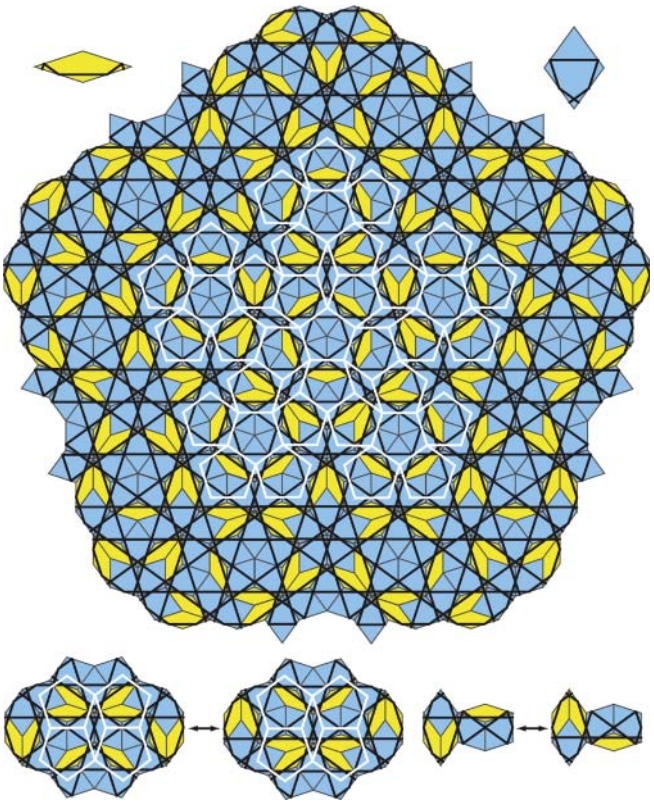

Fig. 6. Penrose tiling (*PT*) with Ammann lines (black). The two unit rhombs are shown (on top) with line segments. In the central part of the rhomb *PT* a pentagonal tiling is shown (white). There are three different decorations of pentagons by rhombs and Ammann lines, respectively. In the lower part of the figure, the flipping of an Ammann line is shown on the example of a larger patch. The flips consist of simpleton flips in the two types of hexagons occurring in the *PT*.

areas in the upper left part of Fig. 5. Cutting the hypercrystal with the physical space inclined with a rational slope (blue line in Fig. 5) gives the *n*/*m*-approximant (in our example $^{2}/_{1}$). Moving the physical space (horizontal line) through the end points of the atomic surface (marked by an arrow) leads to vertex jumps (phason flips) of the type $LS \Leftrightarrow SL$. Projecting the hypercrystal along the inclined broad yellow strips gives the periodic average structure (*PAS*) of the *FS* (Steurer, Haibach, 1999a; Cervellino, Steurer, 2002).

In the 2D description, the 1D *FS* is symmetric around the origin of the 2D lattice. Vertices with distance $\tau^n L$ from the origin come from atomic surfaces centered on 2D-lattice points with perpendicular-space components $\tau^{-n}S$. Consequently, with increasing n the *FS* around these vertices gets closer and closer to mirror symmetry. This is important for the structures produced by local twinning (Fig. 2). In Fig. 6, a pentagonal tiling, produced by local twinning, is superimposed on the rhombic Penrose tiling (*PT*) decorated by Ammann lines. The Ammann lines, infinite straight lines, cut the rhombic unit tiles always in the same way. Their distances follow a *FS*. Since the local mirror planes at the edges of *P*, *P5P*, (*P5P*) 5(*P5P*), ... have distances from the origin increasing with τ^{2n} for the different generations of pentagon aggregates, they are also pseudo-mirror planes of the *FS* mapping the Ammann lines on themselves. The larger n, the closer are the pseudo-mirrors to real mirrors.

Net planes and 'thin' atomic layers (*TALs*)

At each point of a lattice an infinite number of net planes (lattice planes) intersect. Each net plane (*hkl*) is part of an infinite set of parallel net planes {*hkl*} sampling all lattice points. The density of lattice points on a net plane is inversely proportional to the distance d_{hkl} between neighboring planes. In case of a crystal structure, each atom of a unit cell and all translationally equivalent atoms form a lattice. Except for the smallest unit cells, however, the atoms on a net plane of such a lattice will not be in bonding distance to each other. Consequently, atomic planes of this type will not be of any crystal-chemical importance.

Structurally or morphologically important atomic layers can be obtained if neighboring net planes, which are occupied by atoms bonded to each other, are combined to 'thin' atomic layers (*TALs*) (*cf.* Papadopolos *et al.*, 2004). These structurally important *TALs* correspond to the net planes of morphological importance (*MI*) parallel to the periodic bond chains (*PBC*) that form the facets of crystals (Hartman, 1987). Since *TALs* are densely occupied by atoms, they give rise to strong Bragg reflections. These define Brillouin zones or, in case of *QCs*, Jones zones and act as strongly scattering planes for conduction electrons. *TALs* of low *MI* can be favorite growth planes that disappear eventually. *TALs* can

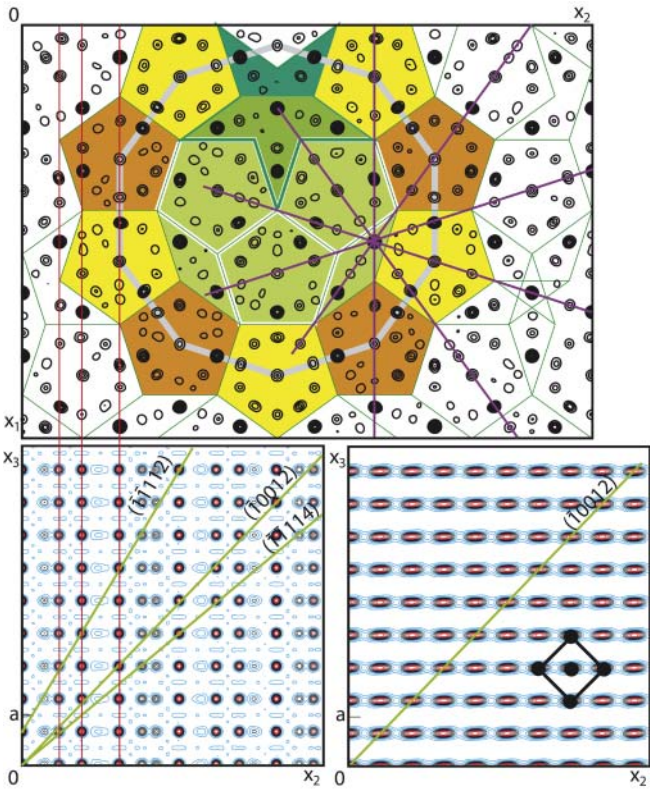

Fig. 7. Structure of decagonal Al−Co−Ni projected upon (11000) (Cervellino, Steurer, 2002) (upper figure) and (01100) (lower left figure) (Steurer, Cervellino, 2001). The *PAS* is shown in the lower right picture. The green lines mark the traces of the net planes inclined to the tenfold direction [00100]. The red lines indicate (10100) planes in the projections of the decagonal structure upon (11000) as well as on (01100). One unit cell of β-$(Co,Ni)_{1-x}Al_{1+x}$ is marked (black) in the *PAS*. The $(\bar{1}0012)$ plane of the *PAS* is parallel to the (010) plane of the β-phase.

also act as glide planes during mechanical deformation of *QCs* and *CMAs*, in general.

Net planes in *QCs* are quasiperiodically spaced. The Ammann lines of a Penrose tiling (*PT*), for instance, can be seen as traces of net planes of a *DQC* (Fig. 6). In *DQCs,* there also exist special sets of net planes, the so called 'inclined net planes', connecting both the periodic and quasiperiodic directions (Steurer, Cervellino, 2001) (Fig. 7). These net planes are lattice planes of the periodic average structure of the *DQC* and form structurally important *TALs.* For the growth of *DQC*, they can play an important role in guiding the growth in the quasiperiodic direction. Some of them have been observed as growth facets (Steurer, Cervellino, 2001; Gille *et al*., 2005). In Fig. 7, it is shown that the $(\bar{1}0012)$ net plane of decagonal Al−Co−Ni corresponds to the $(0\bar{1}1)$ net plane of the *PAS* and is parallel to the (010) plane of the β-phase, $(Co,Ni)_{1-x}Al_{1+x}$.

In the context of surface studies of *QCs*, there is an ongoing discussion on the terminating planes. It has been shown that these should be *TALs* (Papadopolos *et al*., 2004). There seems also to be a tendency to contract *TALs* in the bulk structure. This has been indicated in the structure refinements of *QCs* by small displacements of atoms from positions they should occupy in an ideal quasiperiodic structure in order to form denser *TALs* (see, for instance, Yamamoto, Takakura, 2004; Cervellino, Haibach, Steurer, 2002).

Complex intermetallic phases are usually described either in terms of a cluster packing or in terms of a layer structure (see, for instance, Frank, Kasper, 1958 and 1959). Both points of view can be useful. While the cluster description is focusing on local symmetry and packing considerations, the *TAL* description focuses on long-range order.

The example Al−Co−Ni

Rapid solidification experiments have shown that both $CoAl_3$ and $NiAl_3$ (Grushko, Holland-Moritz, 1997; Pohla and Ryder, 1997) form metastable decagonal phases. Electron diffraction patterns indicate a perfect four-layer structure for decagonal $CoAl_3$ and a perfect two-layer structure for decagonal $NiAl_3$. The diffuse scattering of stable decagonal Al−Co−Ni as a function of the Co/Ni-ratio behaves like a weighted average of the diffraction patterns of the two boundary phases $CoAl_3$ and $NiAl_3$ (Katrych, Steurer, 2004). Annealing of decagonal $NiAl_3$ leads to the appearance of diffuse interlayer lines indicating a twofold superstructure along the tenfold axis, eventually orthorhombic $NiAl_3$ is formed. This continuous transformation process shows a close relationship between the decagonal phase and the β-phase.

Approximants and clusters

Rational *n*/*m*-approximants are the set of structures that can geometrically be derived by a perpendicular space shear of a *QC* in the higher-dimensional description (see Steurer, Haibach, 1999b, and references therein) (Fig. 5). Mostly low-order rational (stable) approximants have been discovered up to now (for a list of approximants in the system Al−Co−Ni, see Steurer, 2004). Approximants in the wider sense of the word posses periodic crystal structures consisting of the same atomic clusters as *QCs*.

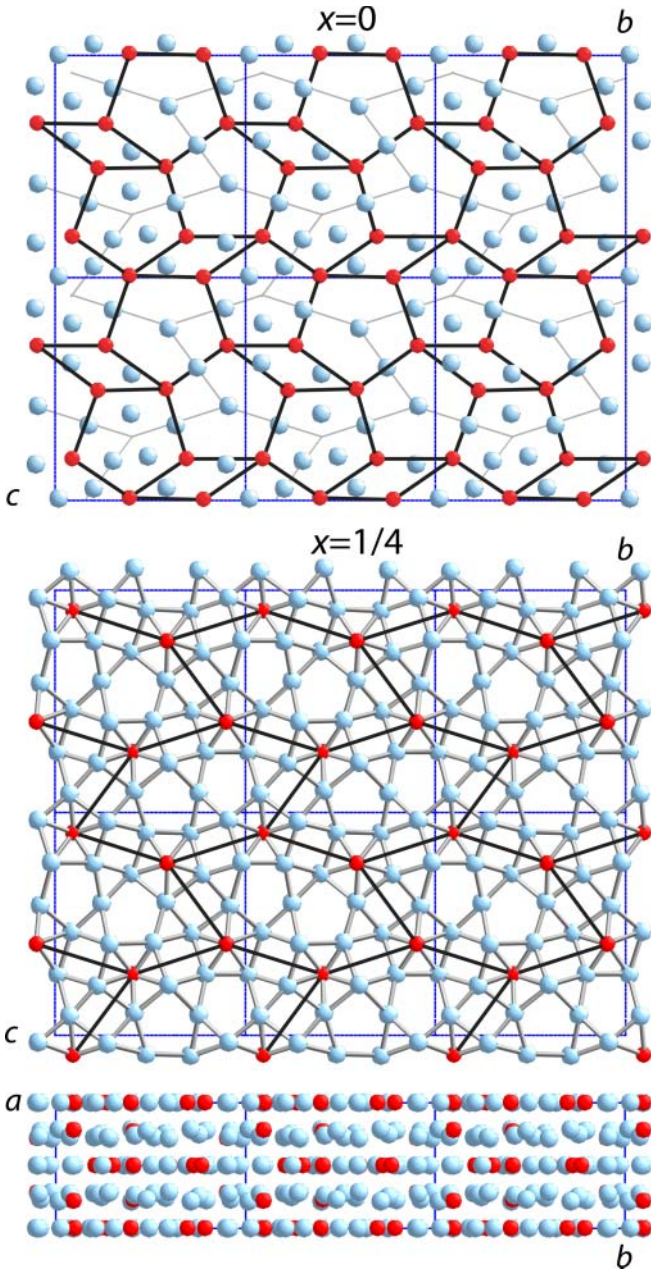

Fig. 8. The structure of $oP102\text{-}Co_4Al_{13}$ (Grin *et al*., 1994) as typical example of a Co-rich approximant and the pentagonal bipyramidal cluster (Al ... blue, Co ... red). Depicted are (011) layers with $x = 0$ and $x \approx {}^1/_4$ as well as the structure projected along [001].

The approximants in the binary system Al−Co are characterized by pentagonal structure motifs and two or four layer periodicity. A typical example is orthorhombic $oP102\text{-}Co_4Al_{13}$ (Grin *et al*., 1994) (Fig. 8). Its four-layer periodicity is a superstructure of the basic two-layer period mainly caused by Al ordering. Considering the framework of Co atoms only, one finds exactly 4 Å periodicity for the subframework of planar pentagon-rhomb layers in $x = 0,\ {}^1/_2$ The slightly puckered hexagon (*H*) layers in $x = {}^1/_4,\ {}^3/_4$ show only minor deviations from 4 Å periodicity. Thus the Co atoms form body-centered pentagonal prismatic columns with 4 Å periodicity in good approximation.

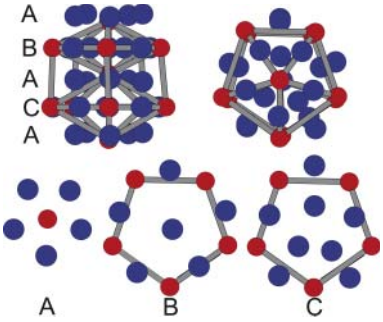

Fig. 9. Structure of the building unit of o*P*102-Co_4Al_{13} (Fig. 8), the double-period pentagonal bipyramidal cluster (*DPPBP*). Layers A are in $x \approx {}^1/_4$, ${}^3/_4$, layer B in $x = 0$, layer C in $x = {}^1/_2$ (Al ... blue, Co ... red).

The fundamental structural unit of all approximants in the system Al−Co is the pentagonal bipyramid (*PBP*, short *P*) or the double-period *PBP* of Co atoms filled with Al atoms (Fig. 9). This type of cluster represents a rather densely packed entity (Cockayne, Mihalkovic, 1999). However, the packing in the approximant is not optimum, strong deviations from regular shape of the *PBPs* are observed. The pentagonal clusters deviate from ideal size and shape even in *DQCs*.

The binary and pseudo-binary Al−Ni and Al−(Co,Ni) approximants are vacancy ordered superstructures of the cubic NiAl β-phase, which itself is related to the *PAS* of decagonal Al−Co−Ni. Thus, the *DQC* may be considered as a compromise between the competing driving forces to form pentagonal structural units on the one side and vacancy ordered superstructures of the NiAl β-phase on the other side. It has been shown that the (110) plane of Ni_2Al_3 is a periodic arrangement of the two unit rhombs of the Penrose tiling (Pohla, Ryder, 1997). Besides these geometrical relationships, it has also been shown that the electronic structures of Al_3Ni_2 and Al(Co,Ni) are similar to that of the decagonal phase (Zurkirch *et al.*, 1998).

It is remarkable that the interatomic distances in the approximants scatter considerably: Al−Al: 2.48–3.20, Al-TM: 2.31–2.69, TM-TM: 2.50–3.15 Å. The β-phase $(Co,Ni)_{1-x}Al_{1+x}$ is with Al-Al: 2.87, Al-TM: 2.49, TM-TM: 2.50 Å closest to the decagonal phase.

The binary Al−Co as well as the ternary Al−Co−Ni approximants consist of the same basic pentagonal bipyramidal structure elements as the *DQC* in different arrangements. The broad stability range of decagonal Al−Co−Ni can be interpreted in terms of entropy gain by Co/Ni substitutional disorder and phasonic disorder of a part of the Al atoms.

The structural differences between the binary and ternary phases in the system Al−Co−Ni as a function of composition are a consequence of the following, partly competing, factors:

1. Within the layers, Co is preferentially 5-coordinated by Al.
2. There is an optimum Co−Co distance of 4–5 Å due to a deep minimum in the Friedel oscillations of the pair potential.
3. Al forms pentagon/rectangle/triangle tilings.
4. Co forms τ-times larger pentagon/rhomb tilings.
5. Co atoms of adjacent layers form dual hexagon tilings.

β-$(Co,Ni)_{1-x}Al_{1+x}$

The β-phase, with a more or less disordered CsCl-structure type, is not a simple Fibonacci-type rational approximant of the *DQC*. It results from the oblique projection of its 5D hypercrystal structure in the *IMS* description (Steurer, 2000). This means, it corresponds to an important *PAS* of the *DQC* related to a special set of strong Bragg reflections.

The lattice parameters of the *PAS* of a *DQC* are

$$\mathbf{a}_1^{PAS} = \pi^{\parallel}(\mathbf{d}_1^{IMS}) = \frac{2}{a_1^*} \begin{pmatrix} \tau^{-1} \\ 0 \\ 0 \end{pmatrix}_V ,$$

$$\mathbf{a}_2^{PAS} = \pi^{\parallel}(\mathbf{d}_2^{IMS}) = \frac{2}{a_1^*} \begin{pmatrix} 0 \\ (3-\tau)^{-1/2} \\ 0 \end{pmatrix}_V ,$$

$$\mathbf{a}_3^{PAS} = \pi^{\parallel}(\mathbf{d}_5^{IMS}) = \frac{1}{a_5^*} \begin{pmatrix} 0 \\ 0 \\ 1 \end{pmatrix}_V .$$

For decagonal Al−Co−Ni with $a_r = 2.456$ Å (Steurer *et al.*, 1993) we obtain

$$a_1^{PAS} = 5a_r/\tau^3 = 2.899 \text{ Å},$$

$$a_2^{PAS} = a_r(3-\tau)^{3/2} = 3.990 \text{ Å},$$

$$a_3^{PAS} = a_3 = 4.0807 \text{ Å}.$$

We can compare these lattice parameters with distances for β-CoAl: $a_{100} = 2.862$ Å, $a_{110} = 4.047$ Å and $a_{1\bar{1}0} = 4.047$ Å. This is indeed a good agreement, which is also shown in Fig. 7. As already pointed out by Dong *et al.* (2001), the angle between the directions [111] and $[11\bar{1}]$ in the structure of β-CoAl is 70.52°, close to the 72° for ideal 5-fold symmetry. The size ratio $r_{Al}/r_{Co} = 1.432/1.253 = 1.143$ (for Ni: 1.149) is far from the optimum radii ratio $r_A/r_B = 1.426$ for a pentagonal arrangement of hard spheres (pentagon edge length $s_5 = 2r_A$) centered by a smaller sphere ($r_B = r_A(1 - \cos 3\pi/10)/(\cos 3\pi/10)$). The ratio of atomic distances in β-CoAl $d_{Al\text{-}Al}/d_{Co-Co} = 2.862/2.479 = 1.155$, however, is pretty close to it. This means, that the atomic distances (bond strengths) in the first coordination sphere of TM atoms are the same in both structural arrangements.

According to Cooper (1963), the maximum lattice parameters for β-CoAl ($a = 2.8619(3)$ Å, point density $PD = 0.0853$ Å^{-3}) and NiAl (a = 2.8864(6) Å, $PD = 0.0832$ Å^{-3}) are obtained for ≈51% Al indicating a slight solubility of Al at the TM sites. With further increasing Al content to 53% and 52.5%, respectively, the lattice parameters decrease by 0.0015 Å and 0.004 Å, respectively due to the increasing number of vacancies at the TM sites. Thus, the increase in Al is mainly relative, it results just from the decrease in TM content. According to Xiao and Baker (1994), however, there is approximately the same amount of Al atoms at TM sites as vacancies.

The Al atom is bigger than the TM atoms are. Putting Al on a TM site generates a rather close contact to 8 other Al atoms. This would be energetically less favorable than the formation of a vacancy in case of Ni and only slightly less favorable for Co (Bester *et al.*, 1999).

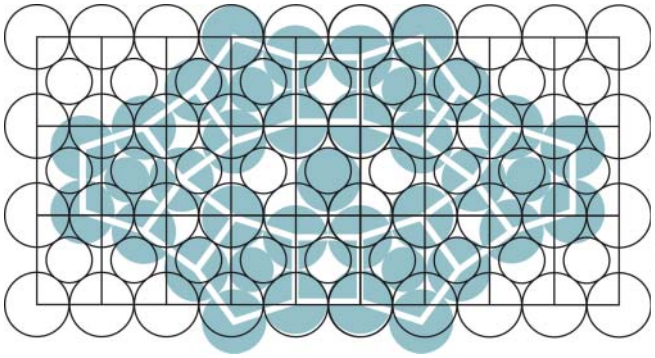

Fig. 10. Pentagonalization of the (110) layer of the CsCl-type structure of the ordered β-phase (open circles). The shifted atoms are marked blue, the typical tiling is drawn in white (compare with Fig. 8, layer in $x \approx 1/4$).

The point density, *PD,* of decagonal Al−Co−Ni is between 0.0661 $Å^{-3}$ (Takakura *et al*., 2001) and 0.0644 $Å^{-3}$ (Cervellino, Steurer, 2002), *i.e.* more than 20% smaller than that of β-CoAl. This is partly due to the larger atomic volume of Al that replaces 40% of the Co sites, partly due to the less efficient packing of the *DQC*. For comparison, the point density of pure *cF*4-Al amounts to 0.0602 $Å^{-3}$, of *cF*4-Ni to 0.0914 $Å^{-3}$ and of *hP*2-Co to 0.0903 $Å^{-3}$. The average point density based on the concentration-weighted atomic volumes results to 0.0722 $Å^{-3}$ for β-CoAl and to 0.0663 $Å^{-3}$ for the decagonal phase $Al_{72.5}Co_{24.5}Ni_3$.

The electron concentration of β-CoAl amounts to e/a = 1.5 electrons/$Å^{-3}$. The binary β-phases have the maximum melting temperature for the 1 : 1 composition (CoAl: at 1200 °C the stability range is from 27 to 53.5% Al, $T_{max} = 1640$ °C vs. $T_m^{Co} = 1495$ °C; NiAl: at 1200 °C the stability range is from 35 to 57.5% Al, $T_{max} = 1638$ °C vs. $T_m^{Ni} = 1455$ °C; Gödecke, 1998). It is remarkable, that the addition of a third component decreases the melting temperature so drastically. The liquidus temperature is decreased to that of the primary crystallization surface of the decagonal phase (Gödecke, 1997). In the binary system Al−Co, at 1180 °C, Co_2Al_5 is formed peritectically from β-CoAl and melt, in the system Al−Ni at 1133 °C, Ni_2Al_3 forms. The lattice parameters of β-(Co,Ni)Al vary linearly with Co/Ni ratio (Kek, 1991).

The β-phase is dominated by strong Al−Co interactions. Each Al atom is 8-coordinated by TM and vice versa. The (110) layers show a pseudo-hexagonal close packing of atoms. Each TM (Al) atom is surrounded by 4 Al (TM) atoms in the distance $a\sqrt{3}/2 = 0.866$ and 2 TM (Al) atoms in the distance a. According to Cooper (1963), the maximum lattice parameter (*i.e.* for 51% Al) for Co−Al is $a = 2.8619(3)$ Å. This is also the Al−Al distance while the Al−Co distance results to 2.479 Å. After pentagonalization (Fig. 10), *i.e.* a distortion of the structure towards the quasiperiodic structure for composition close to that of the *DQC*, the coordination increases to 5 in the distance $a\sqrt{3}/2$.

Geometrical growth model

The characteristic structural unit seen in electronmicroscopic images of *DQCs* is a kind of decorated Gummelt decagon with ≈20 Å diameter (Gummelt, 1996). It has been argued that a quasiperiodic covering based on such a unit has a lower energy than any periodic structure based on it (Jeong & Steinhard, 1994). The open questions are how the overlapping rules are realized on the atomic level and how *QC* growth takes place. In the following a schematic geometrical model is given for the growth of decagonal Al−Co−Ni to illustrate the principles leading to quasiperiodic order.

For the fundamental unit we take a subcluster of the ≈20 Å cluster, the pentagonal bipyramid (*PBP*, short *P*) or a double-period *PBP* consisting of a framework of TM atoms with ≈4.5 Å distance (Fig. 9). This distance corresponds to the second minimum in Co−Co and Ni−Ni pair potentials, respectively (Widom *et al*., 2000). The TM atoms at the tops are regularly pentagonally coordinated by Al atoms. The TM pentagon atoms are either bridged by Al atoms forming a 10-ring or an irregular arrangement. Al atoms are mainly responsible for the 8 Å period as well as for disorder. The driving forces for the formation of a *DQC* are energy minimization by maximizing the packing density of these energetically favorable basic units and entropy maximization by forming structures best suitable for phasonic excitations (phason flips). Additional entropy contributions are provided by chemical disorder (Co/Ni), subtitutional disorder (Al/□) and displacive disorder (puckering of atomic planes). Hume-Rothery-type electronic stabilization keeps *DQC* growth along regular net planes (Ammann type) and inclined net planes (*PAS* type).

It has been shown that placing atoms at sites where four or five lattice lines with relative 5-fold orientations meet (lilac star of five lines in the upper picture of Fig. 7) and at fixed distances from their neighbors generates quasilattices with very little disorder (Olami, 1991). If we replace 'lattice lines' by net planes and 'atoms' by 'atomic clusters' such as *PBP*s then we arrive at our model.

Rapid nucleation is typical for *QC*s. Even rapidly quenched *QCs* ($>10^6$ Ks^{-1}) show correlation lengths of several hundred Å. The first step of quasiperiodic growth must therefore be governed by local parameters, because there is not much time for diffusion and equilibration. In the following, we distinguish two basic mechanisms, pentagrammal growth and β-phase-templated growth, respectively. Pentagrammal growth may be favorable in the primary crystallization regime of the *DQC* where no β-phase exists. If β-phase is already present then heterogeneous nucleation of the *DQC* on the β-phase and β-phase-templated growth can take place.

Decagonal Al−Co−Ni forms peritectically at 1175 °C from β-phase and liquid Al. In the isothermal section at 1170 °C, decagonal $Al_{72.5}Co_{24.5}Ni_3$ is in equilibrium with β-$Al_{55}Co_{35}Ni_{10}$ or, taking into account the structural vacancies, $Al_{51}(Co,Ni)_{42}\square_7$ (Gödecke *et al*., 1998). At 1100 °C, the Ni content of the decagonal phase reaches up to 12.5 at.% and at 900 °C a maximum of 22 at% for 70% Al content.

At certain compositions or for melts that are undercooled by more than 60 K (Liu *et al*., 2002), the *DQC* crystallizes directly from the melt. Consequently, we will discuss in the following two scenarios. The first refers to primary crystallization of the *DQC* from the melt (pentagrammal growth), the second to peritectic formation from β-phase and liquid Al (β-phase-templated growth).

Model of pentagrammal *DQC* growth

Our model assumption is that the primary crystallization of the *DQC* is governed by the following three factors acting on different scales:

1. *primary factor (local)*: spontaneous formation of pentagonal bipyramidal basic clusters (partially already in the melt). Formation of *P5P* clusters: $P + 5P \rightarrow P5P$ (Fig. 2).
2. *secondary factors (local)*: growth by addition of atoms and basic clusters in compliance with local fivefold symmetry and the constraint of extended *TAL* formation. Pentagonal local twinning preserves pentagrammal symmetry. Formation of *P5P* stellated by hexagons, *H*: $P5P + 5P2P \rightarrow (P5P)\,H5 \rightarrow$ relaxation. Completion of peripheral *P2P* clusters: $P2P + 3P \rightarrow P5P$. Formation of superclusters (Gummelt cluster) by rearrangement and relaxation of atoms (Fig. 2).
3. *tertiary factors (global)*: Energy minimization by Fermi-surface nesting. To deepen the pseudo-gap at the Fermi edge, the *TALs* related to the low-index reflections forming the pseudo-Brillouin (Jones) zone have to be compacted, *i.e.* the intensity of the respective Bragg reflections maximized. This means, the *TALs* have to be extended, ordered and as flat as possible. Local 5-fold symmetry extends to global 5-fold symmetry via *TALs* and their scaling symmetry. Further growth is guided by regular *TALs* (along Ammann lines) as well as inclined *TALs* (net planes of the *PAS*). The latter ones form a strong constraint for quasiperiodic growth since it couples the periodic with the quasiperiodic direction.

Model of β-phase-templated *DQC* growth

The structure of the β-phase shows long-range registry with the vertices of an infinite pentagramma (Fig. 11). The farther away from the center of the pentagramma, the closer are the vertices to sites of the β-phase structure. This is a consequence of the scaling properties of the pentagramma in the *n*D description. Scaling in physical space by a factor τ means multiplying its position vector by a factor τ. In perpendicular space this is related to moving the perpendicular space component of its *n*D position vector by a factor $1/\tau$. Thus, the vertex of the pentagramma and the lattice point of the *PAS* get closer and closer to each other by each scaling by a factor τ. Consequently, nucleation starting at points far apart from each other on the β-phase surface is always in registry with the decagonal phase.

Starting from the β-phase, first vacancies order along the [111] directions (τ-phase formation such as Ni_2Al_3, Chattopadhyay *et al.*, 1987). Then Al diffuses into the vacancy-rich structure and preferentially coordinates Co pentagonally. Excess Co/Ni/□ moves to the surface. During this process the β-phase structure distorts locally pentagonally ('pentagonalization') (Fig. 10). Pentagonal bipyramids are formed, interstitial atoms are squeezed out and structural half-vacancies (flip positions) generated.

The pentagrammal symmetry is maintained by local polysynthetic twinning of the *PBPs*. In each pentagramma vertex four net planes meet, a prerequisite of quasiperiodic growth (Olami, 1991). The centers of the pentagons or centering atoms of pentagonal bipyramids form a *HBS* tiling (dual to the pentagon tiling). The TM atoms form the pentagrammal network, Al atoms just act as rather flexible matrix mediating TM-TM interactions (strong sp(Al)-d(TM) interaction).

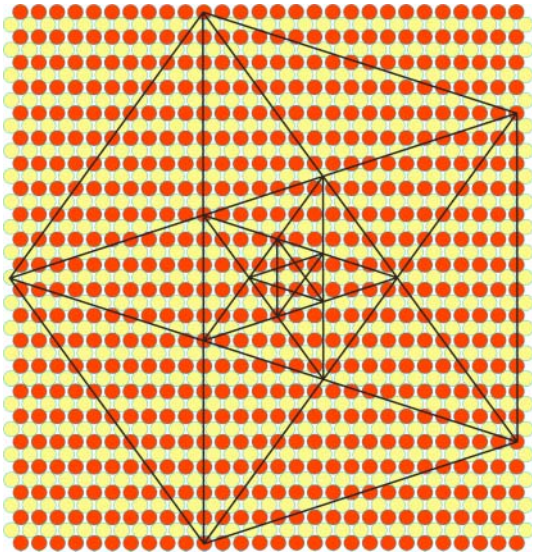

Fig. 11. Pseudo-pentagrammal symmetry of the (110) layer of the CsCl-type structure.

Further growth takes place in a similar way as described in the other scenario.

Conclusions

We have shown two different scenarios for the growth of the decagonal phase in the system Al−Co−Ni. Based on all the previous research done so far in the system Al−Co−Ni (cf. Steurer, 2004) we assume that the cluster picture helps in understanding the formation of *DQCs*. We conclude, however, that the crystal-chemically relevant cluster is much smaller than the usually employed ≈20 Å Gummelt cluster. Moreover, the Gummelt cluster is the result of local twinning of *PBPs*. Consequently, overlapping rules are weak and quasiperiodicity is mainly forced by *TALs,* in particular inclined net planes. In both growth scenarios, the role of *TALs* is crucial for the evolution of long-range-order in the *DQC*.

Our model of polysynthetic local twinning of cluster with *n*-fold symmetry gives a simple geometrical interpretation why only derivative structures of the Penrose tiling (*PT*) have been observed experimentally so far and *QCs* with symmetries such as 7-fold are less likely to be formed.

Future studies will try to prove the ideas presented here, in particular the pentagonalization of the β-phase in the very Al-rich regime, experimentally as well as by quantum-mechanical calculations.

Acknowledgments. Financial support under grant SNF 200020-105158 is gratefully acknowledged.

References

Bester, G.; Meyer, B.; Fähnle, M.: Atomic defects in the ordered compound B2-CoAl: A combination of *ab initio* electron theory and statistical mechanics. Phys. Rev. B**60** (1999) 14492–14495.

Cervellino, A.; Haibach, T.; Steurer, W.: Structure solution of the basic decagonal Al–Co–Ni phase by the atomic surfaces modelling method. Acta Crystallog. B**58** (2002) 8–33.

Cervellino, A.; Steurer, W.: General periodic average structures of decagonal quasicrystals. Acta Crystallogr. A**58** (2002) 180–184.

Chattopadhyay, K.; Lele, S.; Thangaraj, N.; Ranganathan, S.: Vacancy Ordered Phases and One-Dimensional Quasiperiodicity. Acta Metall. **35** (1987) 727–733.

Chen, H. S.; Phillips, J. C.; Villars, P.; Kortan, A. R.; Inoue, A.: New Quasi-Crystals of Alloys Containing s, p, and d Elements. Phys. Rev. B**35** (1987) 9326–9329.

Cockayne, E.; Mihalkovic, M.: Stable quasicrystalline sphere packing. Philos. Mag. Lett. **79** (1999) 441–448.

Cooper, M. J.: An investigation of the ordering of the phases CoAl and NiAl. Philos. Mag. **8** (1963) 805–810.

Cummins, H. Z.: Experimental studies of structurally incommensurate crystal phases. Phys. Rep. **185** (1990) 211–409.

Daams, J.; Villars, P.: Atomic environments in relation to compound prediction. Eng. Appl. Artif. Intell. **13** (2000) 507–511.

Dong, C.; Zhang, L. M.; Belin-Ferre, E.; Brunet, P.; Dubois, J. M.: Surface properties of the B2-based approximants in relation to quasicrystals. Mater. Sci. Eng. A**304** (2001) 172–177.

Dub, O. M.; Chaban, N. F.; Kuz'ma, Yu. B.: New compounds with the structure of YCrB4. Izv. AN SSSR, Neorgan. Mater. **21** (1985) 1967–1968.

Elser, V.: Indexing Problems in Quasicrystal Diffraction. Phys. Rev. B**32** (1985) 4892–4898.

Elser, V.: Random tiling structure of icosahedral quasicrystals. Philos. Mag. B**73** (1996) 641–656.

Frank, F. C.; Kasper, J. S.: Complex alloy structures regarded as sphere packings. I. Definitions and basic principles. Acta Crystallogr. **11** (1958) 184–190.

Frank, F. C.; Kasper, J. S.: Complex alloy structures regarded as sphere packings. II. Analysis and classification of representative structures. Acta Crystallogr. **12** (1959) 483–499.

Gähler, F.; Reichert, M.: Cluster models of decagonal tilings and quasicrystals. J. Alloys Comp. **342** (2002) 180–185.

Gille, P.; Meisterernst, G.; Faber, N.: Inclined net plane faceting observed at Czochralski growth of decagonal AlCoNi quasicrystals. J. Crystal Growth **275** (2005) 224–231.

Gödecke, T.: Schmelzfläche und Phasengleichgewichte mit Beteiligung der Schmelze im System Al–AlCo–AlNi. Z. Metallkd. **88** (1997) 557–569.

Gödecke, T.; Scheffer, M.; Lück, R.; Ritsch, S.; Beeli, C.: Isothermal sections of phase equilibria in the Al–AlCo–AlNi system. Z. Metallkd. **89** (1998) 687–698.

Grin, J.; Burkhardt, U.; Ellner, M.; Peters, K.: Crystal-Structure of Orthorhombic Co_4Al_{13}. J. Alloy. Compd. **206** (1994) 243–247.

Grushko, B.; HollandMoritz, D.: Decagonal quasicrystals in Al–Co, Al–Ni and in their ternary alloys. Mater. Sci. Eng. A**226** (1997) 999–1003.

Gummelt, P.: Penrose tilings as coverings of congruent decagons. Geometr. Dedic. **62** (1996) 1–17.

Guo, J. Q.; Abe, E.; Tsai, A. P.: Stable Cd–Mg–Yb and Cd–Mg–Ca icosahedral quasicrystals with wide composition ranges. Philos. Mag. Lett. **82** (2002) 27–35.

Hartman, P.: In: *Morphology of Crystals*. (Ed. I. Sunagawa), pp. 269–319. Tokyo: Terra Scientific Publishing Company, 1987.

Hu, C. Z.; Ding, D. H.; Yang, W. G.; Wang, R. H.: Possible 2-Dimensional Quasi-Crystal Structures with a 6-Dimensional Embedding Space. Phys. Rev. B**49** (1994) 9423–9427.

Janner, A.: Decagrammal symmetry of decagonal $Al_{78}Mn_{22}$ quasicrystal. Acta Crystallogr. A**48** (1992) 884–901.

Jeong, H. C.; Steinhardt, P. J.: Cluster Approach for Quasi-Crystals. Phys. Rev. Lett. **73** (1994) 1943–1946.

Katrych, S.; Steurer, W.: X-ray diffraction study of decagonal Al–Co–Ni as a function of composition. Z. Kristallogr. **219** (2004) 606–613.

Kek, S.: Untersuchungen der Konstitution, Struktur und thermodynamische Eigenschaften binärer und ternärer Legierungen der Übergangsmetalle mit Aluminium. PhD thesis, University of Stuttgart, Germany (1991).

Kelton, K. F.; Lee, G. W.; Gangopadhyay, A. K.; Hyers, R. W.; Rathz, T. J.; Rogers, J. R.; Robinson, M. B.; Robinson, D. S.: First X-ray scattering studies on electrostatically levitated metallic liquids: Demonstrated influence of local icosahedral order on the nucleation barrier. Phys. Rev. Lett. **90** (2003), art. no.-195504.

Laves, F.: Crystal structure and atomic size. In: *Theory of Alloy Phases.* p. 124. Cleveland. American Society of Metals. 1956.

Levitov, L. S.: Why Only Quadratic Irrationalities Are Observed in Quasi-Crystals. Europhys. Lett. **6** (1988) 517–522.

Liu, X. B.; Yang, G. C.; Fan, J. F.; Wang, J. C.; Song, G. S.: Decagonal quasicrystal formed directly from the undercooled $Al_{72}Ni_{16}Co_{12}$ alloy melt. J. Mater. Sci. Lett. **21** (2002) 367–369.

Luck, J. M.; Godreche, C.; Janner, A.; Janssen, T.: The Nature of the Atomic Surfaces of Quasiperiodic Self-Similar Structures. J. Physics A**26** (1993) 1951–1999.

Olami, Z.: A Local Growth-Process for Quasi-Crystals. Europhys. Lett. **16** (1991) 361–366.

Papadopolos, Z.; Pleasants, P.; Kasner, G.; Fournee, V.; Jenks, C. J.; Ledieu, J.; McGrath, R.: Maximum density rule for bulk terminations of quasicrystals – art. no. 224201. Phys. Rev. B**69** (2004) 4201–4201.

Pelantova, E.; Twarock, R.: Tiles in quasicrystals with cubic irrationality. J. Phys. A**36** (2003) 4091–4111.

Pohla, C.; Ryder, P. L.: Crystalline and quasicrystalline phases in rapidly solidified Al–Ni alloys. Acta Mater. **45** (1997) 2155–2166.

Sato, H.; Toth, R. S.: Effect of additional elements on period of CuAu II and origin of long-period superlattice. Phys. Rev. **124** (1961) 1833–1961.

Sato, H.; Toth, R. S.: Long-period superlattices in alloys. II. Phys. Rev. **127** (1962) 469–484.

Steinhardt, P. J.; Jeong, H. C.; Saitoh, K.; Tanaka, M.; Abe, E.; Tsai, A. P.: Experimental verification of the quasi-unit-cell model of quasicrystal structure. Nature **396** (1998) 55–57.

Steurer, W.: Geometry of quasicrystal-to-crystal transformations. Mater. Sci. Eng. A**294** (2000) 268–271.

Steurer, W.: Twenty years of structure research on quasicrystals. Part 1. Pentagonal, octagonal, decagonal and dodecagonal quasicrystals. Z. Kristallogr. **219** (2004) 391–446.

Steurer, W.; Cervellino, A.: Quasiperiodicity in decagonal phases forced by inclined net planes? Acta Crystallogr. A**57** (2001) 333–340.

Steurer, W.; Haibach, T.: The periodic average structure of particular quasicrystals. Acta Crystallogr. A**55** (1999a) 48–57.

Steurer, W.; Haibach, T.: Crystallography of Quasicrystals. In: Stadnik, Z. M. (Ed.): *Physical properties of Quasicrystals*. Springer, Heidelberg-New York (1999b), pp. 51–89.

Steurer, W.; Haibach, T.; Zhang, B.; Kek, S.; Lück, R.: The Structure of Decagonal $Al_{70}Ni_{15}Co_{15}$. Acta Crystallogr B**49** (1993) 661–675.

Takakura, H.; Yamamoto, A.; Tsai, A. P.: The structure of a decagonal $Al_{72}Ni_{20}Co_8$ quasicrystal. Acta Crystallogr. A**57** (2001) 576–585.

Trambly de Laissadiere, G.; Nguyen-Manh, D.; Mayou, D.: Electronic structure of complex Hume-Rothery phases and quasicrystals in transition metal aluminides. Prog. Mater. Sci. **50** (2005) 679–788.

Weber, S.: Steffen Weber's Home Page (1999) http://www.jcrystal.com/steffenweber/

Widom, M.; Al-Lehyani, I.; Moriarty, J. A.: First-principles interatomic potentials for transition-metal aluminides. III. Extension to ternary phase diagrams. Phys. Rev. B**62** (2000) 3648–3657.

Xiao, H.; Baker, I.: Long range order and defect concentrations in NiAl and CoAl. Acta Metall. Mater. **42** (1994) 1535–1540.

Yamamoto, A.; Takakura, H.: Structure refinement of quasicrystals. Ferroelectrics **305** (2004) 223–227.

Zurkirch, M.; Erbudak, M.; Kortan, A. R.: Electronic-structure analysis of decagonal $Al_{70}Co_{15}Ni_{15}$ by XPS and EELS. J. Electr. Spectr. Rel. Phen. **94** (1998) 211–215.